J Porous Mater (2012) 19:605–613
DOI 10.1007/s10934-011-9511-8

One pot synthesis of cinchona functionalized mesoporous silica and its enantioselectivity

Muhammad Usman Azmat · Yong Guo · Yun Guo · Guanzhong Lu · Yanqin Wang

Published online: 31 August 2011

Abstract Cinchona functionalized mesoporous silica is synthesized by one pot synthesis method. The main silica precursor (TEOS) is co-condensed with a cinchonidine molecule linked organosilane which is renovated by triethoxy silane moiety at its C11 position to yield cinchona functionalized silica. The subsequent deposition of Pt nanoparticles over functionalized silica provides a catalytic system for the enantioselective hydrogenation of α-activated ketone (Orito's reaction). Thus-developed catalyst system is found to be enantioselective with an enantiomeric excess (e.e) of 35.6%.

Keywords Heterogeneous asymmetrical catalysis · Cinchona functionalized silica · Pt/SiO_2-cinchona · Enantioselective hydrogenation · Orito reaction

1 Introduction

Owing to high surface area and tunable pore size, mesoporous silica has numerous applications. A series of significant efforts have been made to incorporate organic components into the inorganic silica frame work to achieve the beneficial properties of the both components to adapt innovative materials that can be used in catalytic systems, to tailor materials for separation operations, optical and electronic devices and many other applications [1–4]. The incorporation of functionalities can be achieved in three ways [5]: by successive attachment of organic components onto a pure silica matrix (grafting) [6–11], by simultaneous reaction of condensable inorganic silica species and silylated organic compounds (co-condensation, one-pot synthesis) [12–15], and by the use of bissilylated organic precursors that lead to periodic mesoporous organosilicas (PMOs) [16–19]. Using grafting route, a great variety of organic groups has been incorporated onto the surface of mesoporous inorganic silica, although usually the incorporation efficiency of the organic functionality to the final material is rather low. The simultaneous co-condensation (one-pot synthesis) of organoalkoxy silanes and the corresponding tetraalkoxy silane precursors have improved the incorporation of different organic moieties [20].

In the field of heterogeneous catalysis, the heterogeneous asymmetric catalysis is of crucial importance as an ever growing demand of enantiomerically pure compounds in the field of life and material sciences has amplified the importance of chiral synthesis [21–24]. Naturally occurring cinchona alkaloids are classified as privileged chiral catalysts [25], having unique chemical structure which can induce chirality to plenty of different achiral compounds and can yield highly pure chiral compounds [26]. The discovery of cinchona-platinum/support catalyst system for Orito reaction (Scheme 1) by the Orito's group [27, 28] has initiated a series of research work in the field of asymmetric hydrogenation of α-functionalized activated ketones and probably the most studied reaction in the field of asymmetric hydrogenation [24, 29–31]. Regarding to this kind of reactions, different research groups have been focused on the role of specific parts of the catalyst systems i.e., the role of supports [32–35], type of metal and its dispersity [36–41], the role of cinchona structure [42–46]

M. U. Azmat · Y. Guo · Y. Guo (✉) · G. Lu · Y. Wang (✉)
Key Lab for Advanced Materials, Research Institute of Industrial Catalysis, East China University of Science and Technology, Shanghai 200237, China
e-mail: yunguo@ecust.edu.cn

Y. Wang
e-mail: wangyanqin@ecust.edu.cn

Scheme 1 Orit's reaction

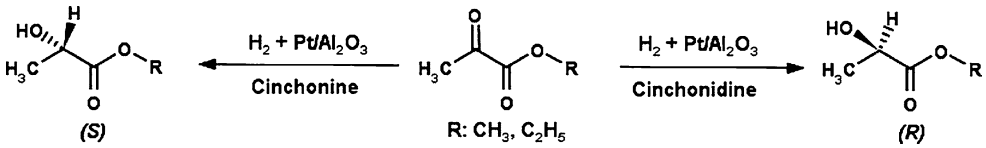

and the working mechanism of cinchonidine (chiral modifier)-substrate over the Pt surface [47–53].

There have been certain reports about the grafting of modified cinchona alkaloids over different supports, including mesoporous silica which has been used in a variety of reactions [54–57]. Recently our group has developed a single unit heterogeneous chiral catalyst system (Pt/SiO_2-cinchonidine) for enantioselective hydrogenation of ethyl pyruvate [57] by using grafting route for direct tethering of cinchonidine molecule to the carboxylate functionalized SBA-15. There are some motivating reports about the synthesis of chiral mesostructured organosilica (ChiMO) which incorporated the chiral ligands in the silica framework by condensing bissilylated chiral organic precursor with a silica precursor [20, 58–62]. Herein, we report probably for the first time the synthesis of cinchona functionalized silica by one pot synthesis method, renovating a cinchonidine molecule to a silylated cinchonidine [63] and further co-condensing with a silica precursor by using cetyl trimethyl ammonium bromide CTAB as a soft template under basic conditions. Pt nanoparticles are deposited afterwards over thus functionalized silica to achieve a package of heterogeneous chiral catalyst system. To our delight, the catalyst system is found to be enantioselective for the Orito's reaction.

2 Experimental

2.1 Materials and method

2.1.1 Reagents

All chemicals were of reagent grade and used as received otherwise mentioned. Cetyl trimethyl ammonium bromide (CTAB), tetraethyl orthosilicate (TEOS), Diethylamine (DEA), NaOH, Tetrahydrofuran (THF), triethylamine (Et_3N), toluene (dried using Na metal and diphenyl ketone), acetic acid, C_2H_5OH, CH_3OH, HCl, formaldehyde (37%) were purchased from Shanghai Lingfeng chemical reagent Co. Ltd; triethoxysilane (EtO_3SiH), cinchonidine 99% and ethyl pyruvate 98% were purchased from Alfa Aesar. Trimethyl chlorosilane (TMSCl) from Sinopharm chemical reagent Co. Ltd., $H_2PtCl_6.6H_2O$ solution Karstedt catalyst (platinum-divinyl tetramethyl disiloxane complex in toluene, 2.1–2.4%Pt) from ABCR GmbH & Co.

2.1.2 Synthesis of cinchonidine functionalized silica by one pot method (CDS-O)

Cinchonidine molecule was modified to create triethoxysilyl functionality at C11 position (Fig. 1) by a reported method [63]. Originally, it involves three synthesis steps, first one is the synthesis of 9-O-(trimethylsilyl) cinchonidine (2 or CDTMS) and second is the synthesis of 9-O-(trimethylsilyl)-11-(triethoxysilyl)-10,11-dihydrocinchonidine (3 or CDTESS) and third is the removal of trimethysilyl group from C9 carbon, the last step was intentionally skipped to keep protecting that C9 chiral position (Scheme 2) which has been reported as of significant role in the enantioselectivity [42–46].

After having silylated cinchonidine CDTESS (confirmed by ^1H NMR) which is a yellowish amorphous material, it need to be dissolved in some organic solvent (toluene and $CHCl_3$) for further condensing with silica source (TEOS) under basic conditions. CTAB was selected as a soft template because it is easy to extract from the organosilica framework as compared to other template i.e., Pluronic P123. We adapted the synthesis method with some modifications as reported earlier [20]. In a typical synthesis, 1.5 g (4.15 mmol) of CTAB was dissolved in 3 g (41.3 mmol) of DEA and 59 g (3.3 mol) of deionized H_2O in a plastic bottle under magnetic stirring at room temperature for 30 min to get homogeneous solution. For CDTESS/TEOS weight ratio as 0.05 (molar ratio CDTESS/TEOS = 0.025), added 5.82 g (27.9 mmol) TEOS and 0.3 g (0.69 mmol) CDTESS (dissolved in either toluene or $CHCl_3$) separately with different time intervals (0–60 min). It is worth mentioning here that we carefully observed that TEOS should be pre hydrolyzed

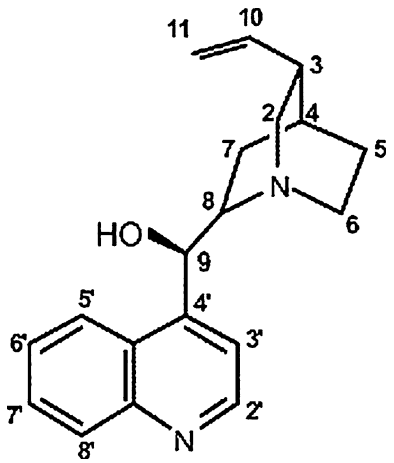

Fig. 1 Cinchonidine molecule with atomic numbering [63]

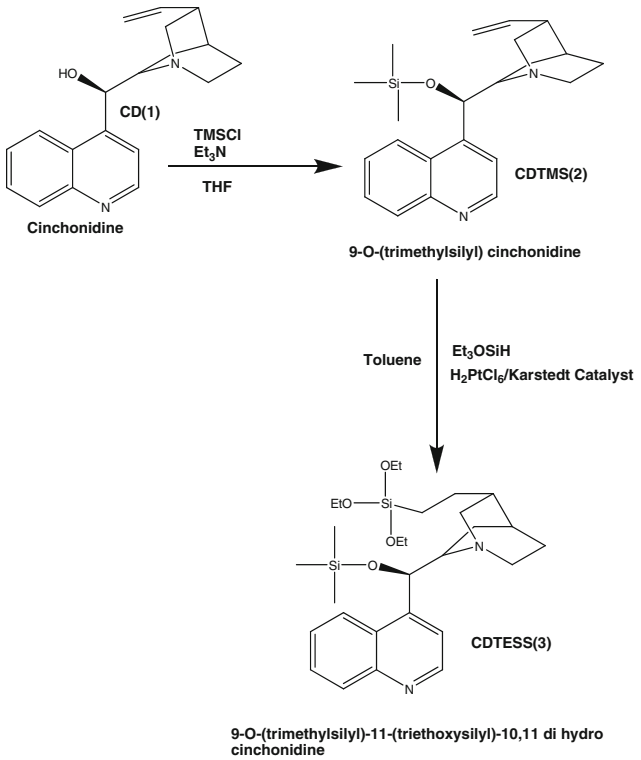

Scheme 2 Steps for prior modification of cinchonidine for triethoxysilylated cinchonidine precursor

before the addition of CDTESS to get some ordered structure. The mixture was further allowed to co-condense under magnetic stirring for 4 h at room temperature. The resultant gel was transferred to an autoclave to be aged statically at 100 °C under autogenous pressure for 48 h. After that the product was filtered, washed with water and ethanol, and dried to get approximately 2.9 g of pale yellow product. To get rid of the template CTAB from the organosilica framework and additionally to remove the protecting group at C9 position of the cinchonidine molecule, 1 g of the dried product was refluxed at 70 °C in 100 mL of CH_3OH and 1.5 mL HCl solution for 8 h, the product was filtered, washed with water and ethanol, and dried to achieve finally 0.8 g of cinchonidine functionalized silica. Thus achieved product was named as $CDS_{t\ or\ c}$-O (time interval for CDTESS addition into prehydrolyzed TEOS solution, CDTESS wt%), where t and c corresponds to toluene and chloroform as co-solvent, respectively. The surface and textural properties were analyzed by XRD and N_2 sorption analysis and organic functionality was determined by FTIR, TG/DTA and CHN elemental analysis.

2.1.3 Pt impregnation over cinchonidine functionalized silica

The deposition–precipitation (DP) method was employed for the impregnation of Pt over cinchonidine functionalized silica (CDS-O) as reported in our previous work [57]. In a typical method, 250 mg of CDS-O was dispersed in 10 mL de-ionized H_2O, then calculated amount (for 3% Pt loading, 0.5 mL) of $H_2PtCl_6.6H_2O$ solution (15 mg/mL) was added and allowed to stir for 2 h at room temperature. Adjusted the pH of the mixture to 10−12 with several drops of 2 M NaOH solution and further stirred for 2 h at room temperature. After that, 3 mL of HCHO solution (37%) was added to reduce Pt ions to Pt particles under refluxing at 100 °C for 1 h till the brownish color appeared, indicating the formation of Pt particles. The product was separated through centrifugation, washed 3 times with de-ionized H_2O and dried to achieve Pt/CDS-O catalyst system for the enantioselective hydrogenation of ethyl pyruvate (EP). The Pt particle size and its dispersion were analyzed by TEM.

2.1.4 Enantioselective hydrogenation of ethyl pyruvate

The hydrogenation of ethyl pyruvate was carried out in a steel reactor equipped with Teflon cylinder and a pressure gauge as reported earlier [57]. In a typical hydrogenation reaction, 30 mg of Pt/CDS-O catalyst was added in the cylinder, to this, 1.5 mL of acetic acid was added as solvent and 75 μL of ethyl pyruvate was used as reactant. H_2 gas was purged several times through the cylinder and then maintained the H_2 gas pressure (0.1 MPa). The reaction was continued for 4 h at 25 °C under magnetic stirring. The product was separated by centrifugation and catalyst was washed with acetic acid (3 times) for further use. The enantioselective product was analyzed by GC-FID with chiral column (CHIRSSIL-DEX CB 25M × 0.25).

2.2 Characterization

X-ray powder diffraction (XRD) patterns were collected on a BRUKER D8 FOCUS using Cu Kα radiation ($\lambda = 1.5404$ Å) operated at 40 kV and 40 mA in the 2θ range of 0.8–5° at scanning rate of 0.6°/min. Nitrogen sorption isotherms were measured at 77 k using NOVA 2020e Quantachrome instrument. Each sample was evacuated at 120 °C for 8 h. The BET surface area was calculated from the adsorption branches in the relative pressure range of 0.05–0.20 and the pore volume was evaluated at a relative pressure of 0.98. The pore diameter and the pore size distribution were calculated from the desorption branch using the Barrett–Joyner–Halenda (BJH) method. The thermogravimetric (TGA) and differential thermal (DTA) analysis were performed concurrently over PerkinElmer Pyris Diamond TG/DTA analyzer, the sample (3–5 mg) was heated in air at a rate of 10 °C/min from 40 to 800 °C. Fourier transform infrared (FTIR) spectroscopy was carried out on Nicolet Nexus 670 FTIR spectrometer

with a resolution of 4 cm^{-1}, the sample was grinded with KBr and then pressed to achieve the pellets. ^1H NMR spectra were recorded at 500 MHz on a Bruker AVANCE 500 spectrometer. CHN contents were determined by Elementar Vario EL III. Transmission electron microscopy (TEM) was performed on FEI Tecnai 20 S-TWIN operating at 200 kV. Enantiomeric excess (e.e) for enantioselective product was calculated as e.e.% = {[R − S]/[R + S]}*100 and measured by GC-FID equipped with a chiral column (CHIRSSIL-DEX CB 25M × 0.25).

3 Results and discussion

3.1 Optimization of the one-pot synthesis step and surface analysis

For the co-condensation of main silica precursor (TEOS) and chiral organic silica precursor (CDTESS), firstly we optimized the hydrolysis time for both TEOS and CDTESS. We observed through experiments that if CDTESS was hydrolyzed prior to TEOS, a non-ordered or less ordered product was achieved. Experimentation was done over the sequence and time of addition of both silica precursors and consequently product was analyzed by XRD and N_2 sorption analysis to find out the proper combination. CDTESS is an amorphous material and it was a necessity to homogenize the chiral organic silica source in a proper organic solvent (co-solvent) prior to co-condensation, toluene and chloroform were selected for that purpose. The resultant product after the condensation was named as CDS_t-O and CDS_c-O for toluene and chloroform when used as co-solvents, respectively. Nature of co-solvent (toluene and chloroform) also affected the surface properties i.e., pore enlargement and loss of ordered structure was observed in some cases when toluene was used. Table 1 summarizes the optimization of the method by describing the conditions for hydrolysis and its effects over the surface properties. It is obvious from Table 1 that when toluene was used as a co-solvent it helps in the enlargement of the pore size as it worked as micelle swelling agent [64]. A predictable trend was also being followed regarding to the orderly structure and the time interval for the addition of CDTESS solution into main solution having TEOS and CTAB. In the case, when CDTESS solution was pre-hydrolyzed 5 min before TEOS (first entry, Table 1), toluene in the solution may have interacted the template CTAB micelle which acted as micelle expander. Afterwards the main silica source TEOS can undergo co-condensation with CDTESS along with other TEOS molecules around the expanded CTAB micelle but not in a very regular fashion and resulted in a non-ordered structure. Afterwards, we tried reverse sequence (TEOS pre-hydrolyzed before CDTESS solution) with different time intervals to achieve an optimum combination, i.e., a larger pore size and moderately ordered structure (entry 4, Table 1). We achieved 5% (weight ratio) cinchonidine functionalized mesoporous silica having 3.25 nm of pore size and moderate ordered structure using toluene as co-solvent. While in case when $CHCl_3$ were used as co-solvent, no pore enlargement phenomenon was observed. The pore size contraction phenomenon was generally observed as we increased the time interval for the addition of CDTESS solution into the prehydrolyzed TEOS solution. The possible reason may be the interaction of co-solvents (toluene or chloroform) with the soft template which was found to be time interval dependant. From the above observations, we analyzed that the hydrolysis rate of CDTESS is higher than that of TEOS and decided to pre-hydrolyze TEOS before CDTESS. Different time intervals for the addition of CDTESS solution were experimented (5, 15, 45 and 60 min) into the pre-hydrolyzed TEOS. From XRD analysis, all thus synthesized chiral organic silica samples were of relatively more ordered structure than those of CDS_t-O (Fig. 2). A slight contraction in pore size was observed when CDTESS contents were raised

Table 1 Optimization of hydrolysis conditions and the surface properties

Sample name	CDTESS/TEOS (weight ratio)	Surface structure[a]	Pore size[b] (nm)	Surface area (m^2/g)
[c]CDS_t-O (−5, 5%)	0.05	Non ordered	4.1	556.4
CDS_t-O (0, 5%)	0.05	Non ordered	3.58	464.3
CDS_t-O (15, 5%)	0.05	Non ordered	3.25	585.3
CDS_t-O (30, 5%)	0.05	Ordered	3.25	591.7
CDS_c-O (5, 5%)	0.05	Ordered	2.83	469.5
CDS_c-O (15, 5%)	0.05	Ordered	2.83	545.5
CDS_c-O (45, 5%)	0.05	Ordered	2.81	567.6
CDS_c-O (45, 7%)	0.07	Ordered	2.76	598.4
CDS_c-O (45, 9%)	0.09	Ordered	2.72	580.8
CDS_c-O (6o, 5%)	0.05	Ordered	2.99	535.7

[a] Surface structure was determined by XRD

[b] Pore size and surface area by N_2 sorption analysis

[c] $DS_{t\ or\ c}$-O (time interval for the addition of CDTESS to prehydrolyzed TEOS)

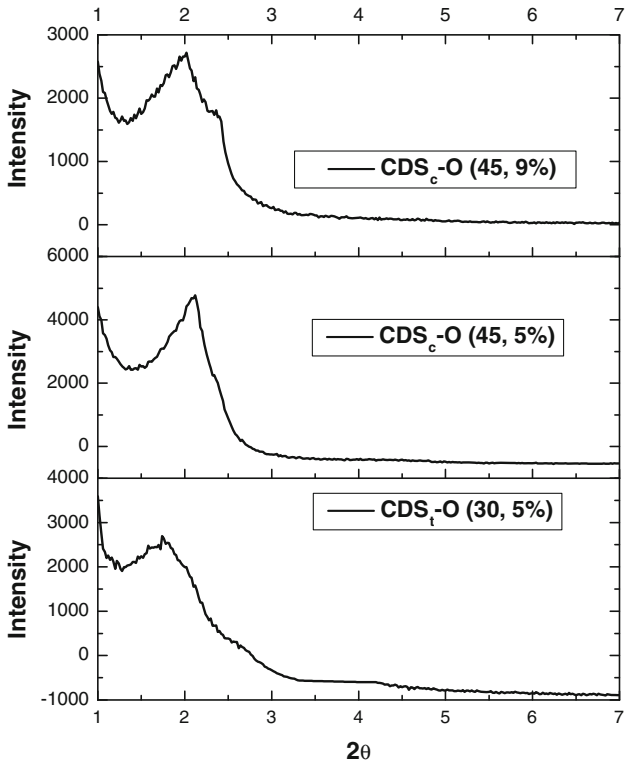

Fig. 2 XRD patterns for synthesized cinchona functionalized silica

from 5 to 9%, but the structure still remain ordered (entry 7, Table 1). The degree of ordering lessens with increasing organic contents (Fig. 2), the XRD peak become more broaden for CDS_c-O (45, 9%) with 9% of CDTESS than for that of 5% for CDS_c-O (45, 5%).

Figure 3 shows the N_2 sorption analysis for CDS_t-O (30, 5%) (i) and CDS_c-O (45, 5%) (ii). Figure 3a represent the N_2 sorption isotherms, curves i and ii correspond to type IV isotherms with characteristic hysteresis loops corresponding to the cylindrical mesopores [65]. Figure 3a, curve i for CDS_t-O (30, 5%) is different in shape because of toluene (co-solvent) effect. Figure 3b reveals that narrow pore size distributions were followed by the above discussed cinchona functionalized silica specimens.

3.2 Organic functionality determination

The ultimate purpose is to functionalize silica with a cinchonidine molecule, which was achieved by co-condensation of the both silica precursors (main silica source as TEOS and chiral silica source as CDTESS). Scheme 3 represents an artistic view of one pot synthesis route to the cinchonidine functionalized silica. The presence of organic functionality over thus synthesized materials is evidenced by CHN elemental analysis, FTIR and TG/DTA analysis.

5, 7 and 9% (based on initial CDTESS/TEOS weight ratio) cinchonidine functionalized silica was also synthesized by one pot synthesis method; the results of CHN analysis are shown in Table 2.

The efficiency of the successful attachment of organic moiety into silica matrix is estimated (taking N contents as a reference for cinchonidine) to be more than 75% based on CHN elemental analysis. Percent efficiency of the method was calculated by using Eq. (1)

$$\%\text{Efficiency} = \left\{\frac{\text{Final loading determined by CHN analysis}}{\text{Initial loading}}\right\} \times 100. \quad (1)$$

Figure 4 shows the FTIR spectra for the as-synthesized and CTAB extracted sample, CDS_c-O (60, 5%). It is obvious from the spectra that soft template CTAB is removed from the organic–inorganic hybrid material as strong C–H stretching (at 2,930 and 2,850 cm^{-1}) and bending (at 1,470 cm^{-1}) bands are vanished after extraction. Some kinks can be observed (black curve Fig. 4) in the stretching and bending C–H band regions which may corresponds to the built-in cinchonidine in the organic–inorganic hybrid material.

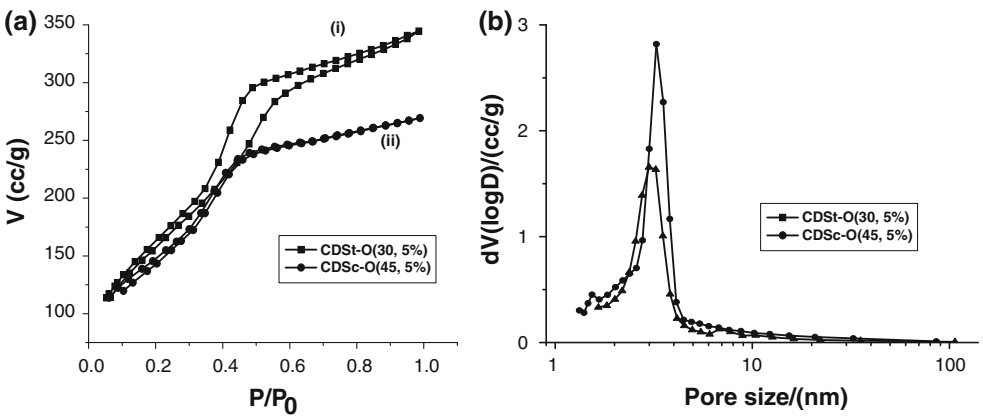

Fig. 3 N_2 sorption isotherms (**a**) and BJH pore size distribution (**b**) for CDS_t-O (30, 5%) and CDS_c-O (45, 5%)

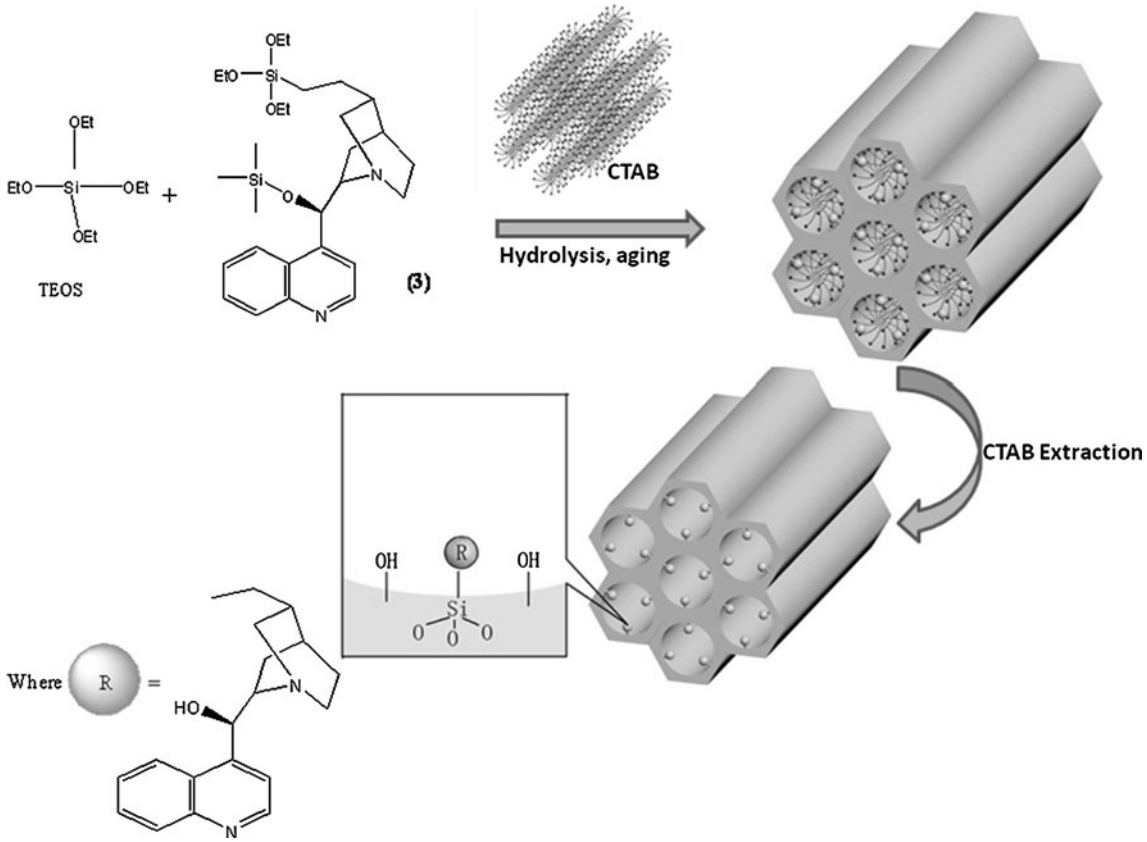

Scheme 3 Schematic representation of one pot synthesis of cinchona functionalized silica (CDS-O)

Table 2 CHN elemental analysis for cinchona functionalized silicas

Sample name	N (%)	C (%)	H (%)
CDSc-O (45, 5%)	0.42	4.95	1.20
CDSc-O (45, 7%)	0.6	6.42	1.83
CDSc-O (45, 9%)	0.69	7.04	2.04

Further, organic functionality was determined by thermo gravimetric analysis. Figure 5 shows TG/DTA curves for CDS_c-O (60, 5%). Figure 5a is the as-synthesized CDS_c-O (60, 5%) having directing agent CTAB in its mesoporous structure, while Fig. 5b shows the TG/DTA curves for CDS_c-O (60, 5%) free of CTAB and having cinchona functionality. The weight loss due to CTAB is almost diminishes in the temperature region of 180–250 °C as clear from the TG curve of Fig. 5b caused by the removal of template, further weight loss from 250–400 °C is caused by decomposition of CDT-ESS molecule and was calculated as 3.43% which is in accordance with that calculated from the CHN elemental analysis. To confirm the characteristic decomposition of a CDTESS molecule, Fig. 5d shows the TG/DTA curves for CDTESS and it is very clear from the TG curve that most of the CDTESS (more than 70%) molecule is decomposed in the temperature range of 250–400 °C. Figure 5c presents the TG/DTA curves for the template free cinchona functionalized silica CDS_c-O (45, 9%) with 9% by weight of CDTESS initial loading. From 250–400 °C, the weight loss is 5.11%, which is also in agreement with the CHN analysis.

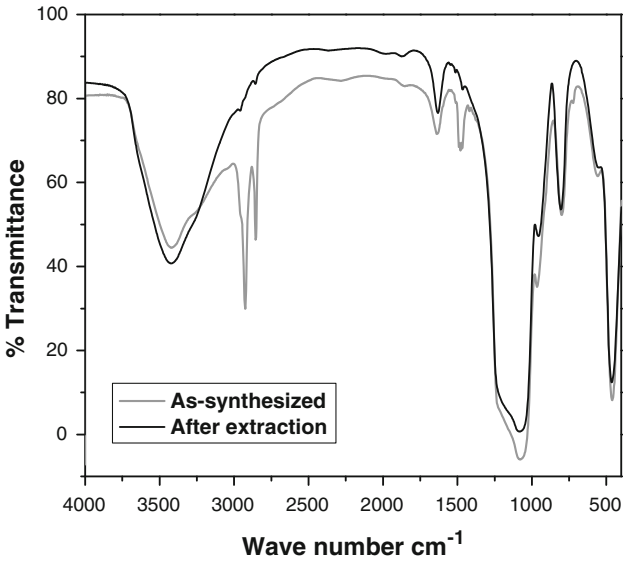

Fig. 4 FTIR spectra for CDS_c-O (60, 5%) as synthesized and after CTAB extraction

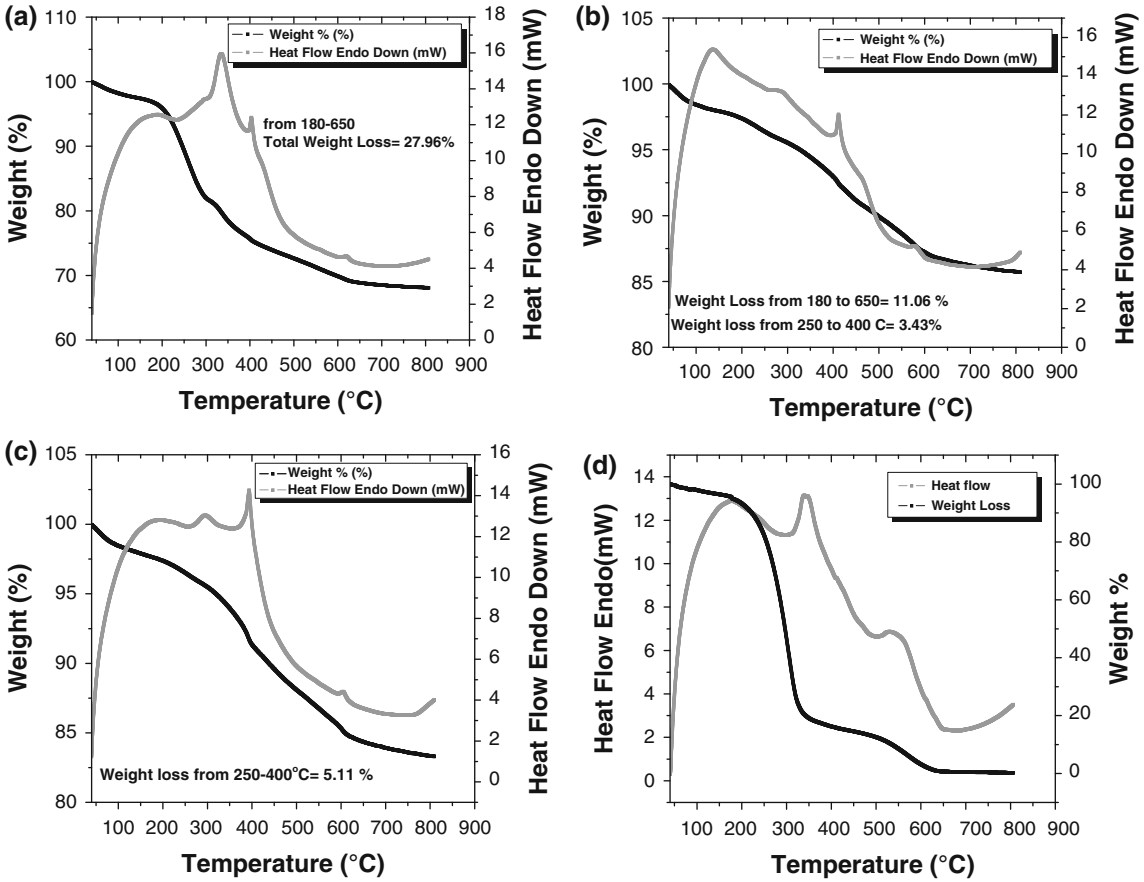

Fig. 5 TG/DTA curves for as-synthesized CDS_c-O(60, 5%) (**a**), after CTAB extraction CDS_c-O (60, 5%) (**b**), CDS_c-O (45, 9%) (**c**) and CDTESS (**d**)

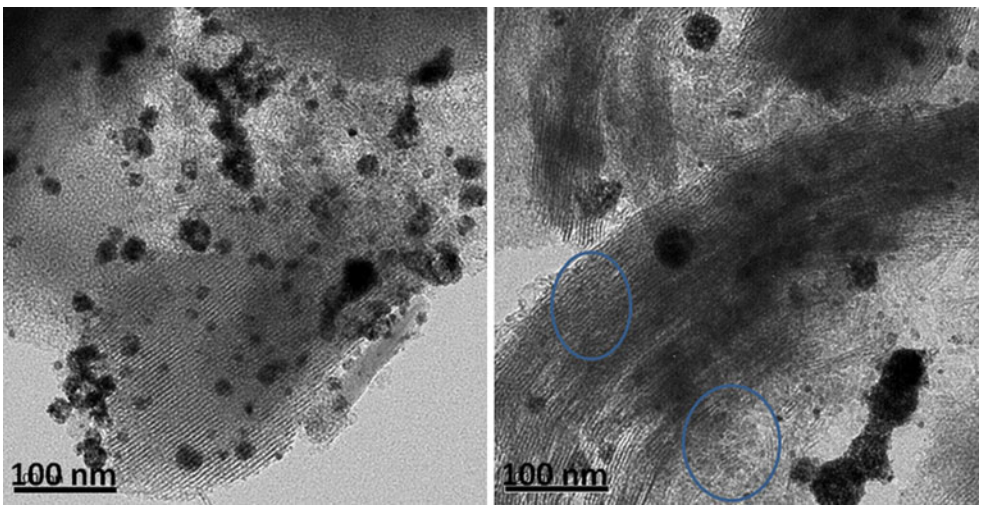

Fig. 6 TEM pictures for CDS-O/Pt

3.3 Catalytic activity

After achieving cinchona functionalized silica, Pt nanoparticles were deposited in/onto the chiral silica to create conducive environment through which enantioselective hydrogenation reaction could be carried out. The Pt nanoparticles are distributed among the pore channels not in a very regular fashion as can be seen from Fig. 6, which cinchona functionalized silica synthesized by one pot method and further deposited by Pt nanoparticles (CDS-O/Pt). It is obvious

Scheme 4 Model reaction of hydrogenation of ethyl pyruvate

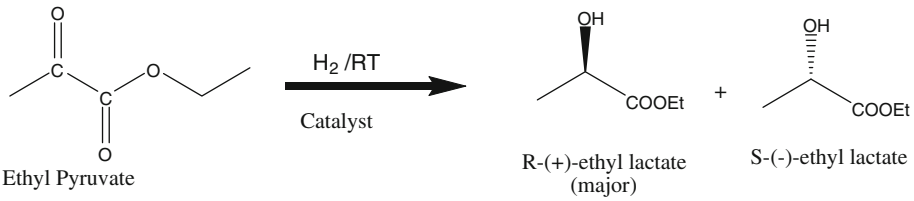

Ethyl Pyruvate

R-(+)-ethyl lactate (major)

S-(-)-ethyl lactate

Table 3 Catalytic activity test for enantioselective hydrogenation of ethyl pyruvate

Catalyst system	Conversion (%)	e.e (%) (R-isomer)
[a]CDS_t-O(−15, 5%)/Pt	100	12.6
CDS_t-O(0, 5%)/Pt	100	17.5
CDS_t-O(15, 5%)/Pt	100	18.9
CDS_t-O(30, 5%)/Pt	100	21.6
CDS_c-O(5, 5%)/Pt	100	24.3
CDS_c-O(15, 5%)/Pt	100	29.7
CDS_c-O(45, 5%)/Pt	100	31.8
CDS_c-O(45, 7%)/Pt	100	35.6
CDS_c-O(45, 9%)/Pt	100	35.2
CDS_c-O(60, 5%)/Pt	100	34.9

[a] 3% Pt contents were loaded over the cinchona functionalized silica

Reaction conditions were optimized at: H_2 pressure = 0.1 MPa, Temp. = Room temp. (17 °C), Time = 4 h, catalyst = 30 mg, ethyl pyruvate = 75 μL, acetic acid (solvent) = 1.5 mL

Table 4 Catalyst recyclability

Catalyst	Conversion (%)	e.e (%) (R isomer)
CDS_c-O (45, 7%)/Pt		
Fresh	100	35.6
Recycle 1	100	34.9
Recycle 2	100	36.1
Recycle 3	100	35.4

that Pt particle distribution is not much harmonized, may be because of more homogeneity of hydrophobic contents (CDTESS) within the silica frame work. As it can be seen from Fig. 6 that some of the Pt nanoparticles (≈2 nm shown as encircled) are residing inside the pore channels which may offer chiral catalytic sites for enantioselective hydrogenation of ethyl pyruvate (EP) if cinchonidine molecules are available in its surroundings. While most of the Pt nanoparticles (>3 nm, larger than pore size) were accumulated onto the silica surface which may contribute to the racemic product if there is no chiral modifier (cinchonidine) in the surroundings.

3.3.1 Hydrogenation of ethyl pyruvate

The catalyst system prepared by cinchona functionalization of silica by one pot method followed by the Pt nanoparticles deposition was tested for a model reaction (Scheme 4) of enantioselective hydrogenation of ethyl pyruvate. The results are summarized in Table 3.

The enantioselectivity was determined for two types of synthesized chiral functionalized silica i.e., CDS_t-O, CDS_c-O (by one pot method, using toluene and trichloromethane as co-solvents, respectively). The catalyst system based on CDS_t-O/Pt was found to be the least enantioselective (Table 3, entry 1–4) but with the 100% conversion. The lower enantioselectivity may be attributed to the poor surface structure which makes the catalysts system unproductive. Comparatively, better enantioselectivities were observed for the catalyst system based on CDS_c-O/Pt ranging from 24.3 to 35.6% of enantiomeric excess (e.e). It has also been observed that increasing the chiral organic contents from 5 to 7% (based on initial loadings) favorably enhances the e.e value (Table 3, entry 8), but further increase to 9% was found not to be very effective (Table 3, entry 9). From this, we can say that catalyst system based on chiral functionalized silica developed by one pot method and further impregnated by Pt nanoparticles, is capable of inducing enantioselectivity in the Orito's reaction.

Catalyst systems based on cinchona functionalized silica synthesized by one pot method and subsequently loaded by Pt nanoparticles were found to be recyclable for at least three times with slight fluctuations in enantioselectivity as shown in Table 4.

4 Conclusions

One pot synthesis method was employed for the synthesis of cinchona functionalized silica. TEOS was co-condensed with a chiral organic silica precursor (CDTESS) under basic conditions and using CTAB as soft template. Thus achieved chiral silica was impregnated by Pt nanoparticles to get a catalyst system CDS-O/Pt which is capable of inducing enantioselectivity to the Orito's reaction.

Acknowledgments This project was supported financially by the 973 Program of China (2010CB732300), the National Natural Science Foundation of China (No. 20973058), the Commission of Science and Technology of Shanghai Municipality (10XD1401400) and the "Excellent scholarship" of East China University of Science and Technology, China. M. U. A. acknowledges the financial support from Higher Education Commission (HEC) of Pakistan for his Ph.D. studies. Authors also thank Prof. Zhenshan Hou and Mrs. Han for their valuable discussions and support throughout the project.

References

1. S. Jayasundera, M.C. Burleigh, M. Zeinali, M.S. Spector, J.B. Miller, W. Yan, S. Dai, M.A. Markowitz, J. Phys. Chem. B **109**, 9198 (2005)
2. B.D. Hatton, K. Landskron, W. Whitnall, D.D. Perovic, G.A. Ozin, Adv. Funct. Mater. **15**, 823 (2005)
3. B. Rác, P. Hegyes, P. Forgo, A. Molnár, J. Appl. Catal. A: Chem. **299**, 193 (2006)
4. J.A. Melero, J. Iglesias, J.M. Arsuaga, J. Sainz-Pardo, P. de Frutos, S. Blázquez, J. Mater. Chem. **17**, 377 (2007)
5. F. Hoffmann, M. Cornelius, J. Morell, M. Froba, Angew. Chem. Int. Ed. **45**, 3216 (2006)
6. N.K. Mal, M. Fujiwara, Y. Tanaka, Nature **421**, 350 (2003)
7. T. Yokoi, H. Yoshitake, T. Tatsumi, J. Mater. Chem. **14**, 951 (2004)
8. A. Walcarius, M. Etienne, B. Lebeau, Chem. Mater. **15**, 2161 (2003)
9. H. Yoshitake, T. Yokoi, T. Tatsumi, Chem. Mater. **14**, 4603 (2002)
10. A.M. Liu, K. Hidajat, S. Kawi, D.Y. Zhao, Chem. Commun. **13**, 1145 (2000)
11. C. Lei, Y. Shin, J. Liu, E.J. Ackerman, J. Am. Chem. Soc. **124**, 11242 (2002)
12. S.L. Burkett, S.D. Sims, S. Mann, Chem. Commun. **11**, 1367 (1996)
13. D.J. Macquarrie, Chem. Commun. **16**, 1961 (1996)
14. M.H. Lim, C.F. Blanford, A. Stein, J. Am. Chem. Soc. **119**, 4090 (1997)
15. L. Mercier, T.J. Pinnavaia, Chem. Mater. **12**, 188 (2000)
16. T. Asefa, M.J. MacLachlan, N. Coombs, G.A. Ozin, Nature **402**, 867 (1999)
17. S. Inagaki, S. Guan, Y. Fukushima, T. Ohsuna, O. Terasaki, J. Am. Chem. Soc. **121**, 9611 (1999)
18. C. Yoshina-Ishii, T. Asefa, N. Coombs, M.J. MacLachlan, G.A. Ozin, Chem. Commun. **24**, 2539 (1999)
19. B.J. Melde, B.T. Holland, C.F. Blanford, A. Stein, Chem. Mater. **11**, 3302 (1999)
20. A.G. Rafael, G. Rafael van, I. Jose, M. Victoria, G. Daniel, Chem. Mater. **20**, 2964 (2008)
21. M. Tada, Y. Iwasawa, Chem. Commun. **27**, 2833 (2006)
22. S.E. Gibson, M.P. Castaldi, Chem. Commun. **29**, 3045 (2006)
23. J.M. Notestein, A. Katz, Chem. Eur. J. **12**, 3954 (2006)
24. E. Talas, J.L. Margitfalvi, Chirality **22**, 3 (2010)
25. P.Y. Tehshik, N.J. Eric, Science **299**, 1691 (2003)
26. K. Kacprzak, J.S. Gawron, Synthesis **7**, 961 (2001)
27. Y. Orito, S. Imai, S. Niwa, J. Chem. Soc. Jpn. **8**, 1118 (1979)
28. Y. Orito, S. Imai, S. Niwa, G.H. Nguyen, J. Synth. Org. Chem. Jpn. **37**, 173 (1979)
29. T. Mallat, E. Orglmeister, A. Baiker, Chem. Rev. **107**, 4863 (2007)
30. M. Bartok, Chem. Rev. **110**, 1663 (2010)
31. H.U. Blaser, M. Studer, Acc. Chem. Res. **40**, 1348 (2007)
32. M. Heitbaum, F. Glorius, I. Escher, Angew. Chem. Int. Ed. **45**, 4732 (2006)
33. T.J. Hall, J.E. Halder, G.J. Hutchings, R.L. Jenkins, P. Johnston, P. McMorn, P.B. Wells, R.P.K. Wells, Top. Catal. **11**, 1–351 (2000)
34. U. Bohmer, K. Morgenschweis, W. Reschetilowski, Catal. Today **24**(1–2), 195 (1995)
35. U. Bohmer, F. Franke, K. Morgenschweis, T. Bieber, W. Reschetilowski, Catal. Today **60**(3–4), 167 (2000)
36. Y. Huang, J. Chen, H. Chen, R. Li, Y. Li, L. Min, X. Li, J. Mol. Catal. A:Chem. **170**(1–2), 143 (2001)
37. H.U. Blaser, H.P. Jalett, Stud. Surf. Sci. Catal. **78**, 139 (1993)
38. H.U. Blaser, H.P. Jalett, D.M. Monti, J.F. Reber, J.T. Wehrli, Stud. Surf. Sci. Catal. **41**, 153 (1988)
39. K. Borszeky, T. Burgi, Z. Zhaohui, T. Mallet, A. Baiker, J. Catal. **187**, 160 (1999)
40. M. Bartok, *Stereochemistry of Heterogeneous Metal Catalysis* (Wiley, New York, 1985)
41. J.T. Wehrli, A. Baiker, D.M. Monti, H.U. Blaser, J. Mol. Catal. **61**, 2–207 (1990)
42. H.U. Blaser, H.P. Jalett, W. Lottenbach, M. Studer, J. Am. Chem. Soc. **122**, 12675 (2000)
43. T. Heinz, G. Wang, A. Pfaltz, B. Minder, M. Schürch, T. Mallat, A. Baiker, Chem. Commun. **14**, 1421 (1995)
44. M. Bartok, K. Balazsik, T. Bartok, Catal. Lett. **73**, 2–127 (2001)
45. A. Solladie-Cavallo, C. Marsol, F. Garin, Tetrahedron Lett. **43**(27), 4733 (2002)
46. A. Pfaltz, T. Heinz, Top. Catal. **4**, 3–229 (1997)
47. M. Bartok, K. Felfoldi, B. Torok, T. Bartok, Chem. Comm. **23**, 2605 (1998)
48. D. Ferri, T. Burgi, A. Baiker, Chem. Comm. **13**, 1172 (2001)
49. M. Bartok, M. Sutyinszki, K. Felföldi, G. Szollosi, Chem. Comm. **10**, 1130 (2002)
50. N. Bonalumi, A. Vargas, D. Ferri, T. Burgi, T. Mallat, A. Baiker, J. Am. Chem. Soc. **127**, 8467 (2005)
51. S. Lavoie, M. Laliberte, I. Temprano, P.H. McBreen, J. Am. Chem. Soc. **128**, 7588 (2006)
52. Z. Ma, F. Zaera, J. Am. Chem. Soc. **128**, 16414 (2006)
53. F. Hoxha, L. Konigsmann, A. Vargas, D. Ferri, T. Mallat, A. Baiker, J. Am. Chem. Soc. **129**, 10582 (2007)
54. B.M. Kim, K.B. Sharpless, Tetrahedron Lett. **31**(21), 3003 (1990)
55. R. Alvarez, M.A. Hourdin, C. Cave, J. d'Angelo, Tetrahedron Lett. **40**(39), 7091 (1999)
56. B. Thierry, J.C. Plaquevent, D. Cahard, Tetr. Asym. **14**, 12–1671 (2003)
57. M.U. Azmat, Y. Guo, Y. Guo, Y. Wang, G. Lu, J. Mol. Cat. A: Chem. **336**, 42 (2011)
58. C. Baleizao, B. Gigante, D. Das, M. Alvaro, H. Garcia, A. Corma, Chem. Comm. **15**, 1860 (2003)
59. C. Baleizao, B. Gigante, D. Das, M. Alvaro, H. Garcia, A. Corma, J. Catal. **223**, 106 (2004)
60. M. Benitez, G. Bringmann, M. Dreyer, H. Garcia, H. Ihmels, M. Waidelich, K. Wissel, J. Org. Chem. **70**, 2315 (2005)
61. D. Jiang, Q. Yang, H. Wang, G. Zhu, J. Yang, C. Li, J. Catal. **239**, 65 (2006)
62. R.A. Garcia, R. Grieken van, J. Iglesias, V. Morales, N. Villajos, J. Catal. **274**, 221 (2010)
63. A. Lindholm, P. Mäki-Arvela, E. Toukoniitty, T.A. Pakkanen, J.T. Hirvi, T. Salmi, D.Y. Murzin, R. Sjöholm, R. Leino, J. Chem. Soc. Perkin Trans. 1 **23**, 2605 (2002)
64. C. Liang, M. Tiffany, K. Michal, Chem. Mater. **21**, 1144 (2009)
65. IUPAC, Reporting Physisorption Data for Gas/Solid Systems, Pure Appl. Chem. **54**(11), 2201 (1982)